

Results on $B_{s,d} \rightarrow \mu\mu$ decays and measurement of P_5' and P_1 parameters in $B_0 \rightarrow K^* \mu\mu$ decay

Stefano Lacaprara^{*†}

INFN Padova

E-mail: stefano.lacaprara@pd.infn.it

Phenomena beyond the standard model (SM) can manifest themselves indirectly, by affecting the production and decay of SM particles.

The features of $B_{d,s} \rightarrow \mu\mu$ decays are sensitive probes of physics beyond the Standard Model. This talk will review the results on these decays from the data collected by the CMS experiment. The decay $B_0 \rightarrow K^* \mu\mu$ is a flavor-changing neutral current (FCNC) process particularly sensitive to new physics, since it is heavily suppressed in the SM. Recent results from LHCb collaboration show a tension with respect to SM prediction of more than 3 sigmas, and the Belle Collaboration reported a discrepancy almost as large. We will present results of an angular analysis done by the CMS experiment at the LHC, using p-p data collected at $\sqrt{s} = 8$ TeV, corresponding to an integrated luminosity of $L = 20 fb^{-1}$. The analysis is focused to measure the angular parameter P_5' , as well as P_1 , as a function of the di-muons invariant mass.

EPS-HEP 2017, European Physical Society conference on High Energy Physics

5-12 July 2017

Venice, Italy

^{*}Speaker.

[†]on behalf of the CMS collaboration

1. Introduction

Phenomena beyond the standard model (SM) of particle physics can become manifest directly, via the production of new particles, or indirectly, by modifying the production and decay properties of particles in the standard model (SM) of particle physics. Analyses of flavor changing neutral current (FCNC) decays are particularly sensitive to the effects of new physics because these decays are highly suppressed in the SM, and new physics can affect the loop through which these decay happens. Among the many examples, two are of particular interest: the leptonic decay $B_s^0(B^0) \rightarrow \mu\mu$ and that of $B^0 \rightarrow K^*\mu\mu$. The two decays are experimentally accessible to the CMS experiment at the LHC, with two muons to allow the trigger of the event, and a fully charged final state.

The first decays are expected to be very rare in the standard model (SM) of particle physics because they are also Cabibbo- and helicity-suppressed. The predicted decay-time integrated branching fractions are $\mathcal{B}(B_s^0 \rightarrow \mu\mu) = (3.65 \pm 0.23) \cdot 10^{-9}$ and $\mathcal{B}(B_d^0 \rightarrow \mu\mu) = (1.06 \pm 0.09) \cdot 10^{-10}$ [1]. The two decays offer very high sensitivity to models with extended Higgs-boson sectors [2, 3, 4, 5].

The second decay $B^0 \rightarrow K^*\mu\mu$, where K^* indicates the $K^{*0}(892)$ meson, has a fully charged final state which allows an angular analysis as a function of the dimuon invariant mass squared (q^2). New physics can modify the values of some angular parameters [6, 7, 8] relative to their SM values [9, 10, 11, 12, 13]. While previous measurements of some of these parameters, by the BaBar, Belle, CDF, CMS, and LHCb experiments, were found to be consistent with the SM [14, 15, 16, 17, 18, 19], the LHCb Collaboration recently reported [20] a discrepancy larger than 3 standard deviations with respect to the SM for the so-called P_5' parameter [21], and the Belle Collaboration reported [22] a discrepancy almost as large.

Here we present the analysis of $B_s^0(B^0) \rightarrow \mu\mu$ decay using pp collision at 7(8) TeV collected by the CMS collaborations at the LHC with an integrated luminosity $L = 5(20) \text{ fb}^{-1}$. Also the results on P_5' and P_1 parameters for the angular analysis of $B^0 \rightarrow K^*\mu\mu$ are presented, using the 8 TeV dataset with $L = 20 \text{ fb}^{-1}$. More details on the two analysis can be found in [23, 24] and [25, 26], respectively. A detailed description of the CMS detector, together with a definition of the coordinate system used and the standard kinematic variables, can be found in Ref [27].

2. Search for $B_s^0 \rightarrow \mu\mu$

The signal $B_s^0/B^0 \rightarrow \mu\mu$ is characterized by two muons from one well-reconstructed secondary B vertex, with the dimuon momentum aligned with the flight direction (from the primary vertex to the B vertex), the dimuon invariant mass around the B pole mass, and isolated dimuons (because the two muons are the only decay particles of the B meson). The background has different components. The combinatorial one, estimated from data side bands; from rare B decays ($B_s^0 \rightarrow K^-\mu\nu$, $\Lambda_b \rightarrow p\mu\nu$) estimated from simulated events; and peaking ($B^0 \rightarrow KK, K\pi, \pi\pi$) whose absolute yield is evaluated on independent single- μ trigger. The signal selection is based on strict requirement for muon identification quality, using MVA technique, good secondary vertex reconstruction, an isolation requirement with respect other tracks in the event, and a selection on the B pointing angle. The excellent muon identification and resolution of the CMS detector allow for a powerful background rejection in the $M_{\mu\mu}$ invariant mass distribution.

The $B^\pm \rightarrow J/\psi K^\pm \rightarrow \mu\mu K^\pm$ decay is used as normalization channel, taking into account the acceptance, trigger, and reconstruction efficiencies, as well as the B fragmentation fraction ratio f_s/f_u [28]. The B^0 and B_s^0 yields are extracted via an unbinned maximum likelihood fit using several categories of events based on data-taking period and events classification.

The results are shown in fig. 1 and the branching fraction for the two decays are the following: $\mathcal{B}(B_s^0 \rightarrow \mu\mu) = (3.0_{-0.8}^{+0.9}(\text{stat.})_{-0.4}^{+0.6}(\text{syst.})) \times 10^{-9}$ and $\mathcal{B}(B_d^0 \rightarrow \mu\mu) = (3.5_{-1.8}^{+2.1}(\text{stat.} + \text{syst.})) \times 10^{-10}$. The observed significance is 4.3 and 2.0 σ , respectively. Given the low significance of B_d^0 decay, an upper limit of $\mathcal{B}(B_d^0 \rightarrow \mu\mu) < 1.1 \cdot 10^{-9}$ at 95% CL is set.

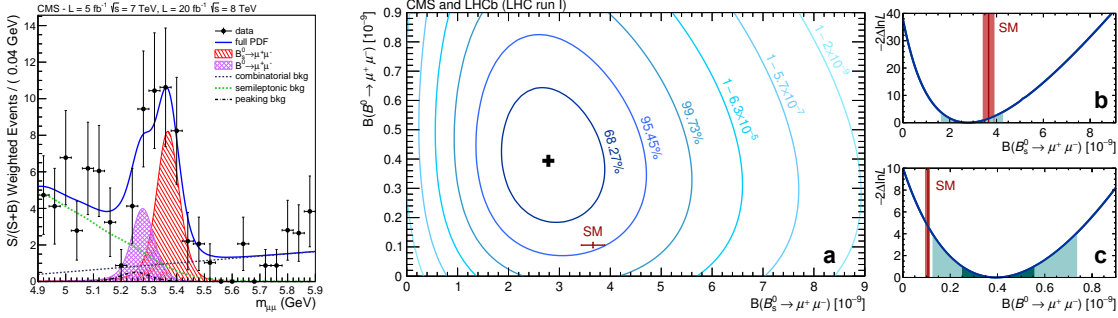


Figure 1: (left) Di-muon invariant mass for combination of all CMS categories. Individual categories are weighted with $S/(S+B)$, where S (B) is the signal (background) determined at the B^0 peak position [23]. (right) Combined results for CMS and LHCb for $\mathcal{B}(B_s^0/B_d^0)$ compared with SM prediction [24].

A combined analysis of the CMS results together with a similar one by the LHCb collaboration [29] provide the following results: $\mathcal{B}(B_s^0 \rightarrow \mu\mu) = (2.8_{-0.6}^{+0.7}) \cdot 10^{-9}$ and $\mathcal{B}(B_d^0 \rightarrow \mu\mu) = (3.9_{-1.4}^{+1.6}) \cdot 10^{-10}$, with a combined significance of 6.2 (7.4 expected) and 3.2 σ (0.8 exp.).

A similar analysis have been published also by ATLAS [30], with comparable, although less sensitive, results, and updated by LHCb, including also a measurement of B_s lifetime [31].

3. $B^0 \rightarrow K^* \mu\mu$ angular analysis

The FCNC decay $B^0 \rightarrow K^* \mu\mu \rightarrow K^+ \pi^- \mu^+ \mu^-$ has a four body, charged final state which can be completely reconstructed. The decay topology is fully described by three angles and the di-muon invariant mass squared $q^2 = M_{\mu\mu}^2$. In this analysis, seven bins of q^2 have been used, in the range 1 to 19 GeV^2 . The three angles, θ_ℓ , θ_K , ϕ , are described in fig. 2. The initial state B^0 (\bar{B}^0) can be identified via K and π charges.

For several parameters of the angular distribution robust SM prediction are available: some of these parameters have been measured by CMS [26], including the forward-backward asymmetry of the muons, A_{FB} , longitudinal polarization fraction of the K^* , F_L , and the branching fraction as a function of q^2 , $d\mathcal{B}/dq^2$, all in good agreement with SM prediction. The same dataset is here used to determine the two parameters P'_5 and P_1 , which are combinations of Wilson coefficient of the effective hamiltonian [32].

The event are selected with a trigger requiring two opposite charged muons from a displaced vertex, with $p_T > 3.5 \text{ GeV}$ and $|\eta| < 2.2$, with $p_T^{\mu\mu} > 6.5 \text{ GeV}$, and with line of flight aligned with the dimuon momentum: $\cos \alpha > 0.9$.

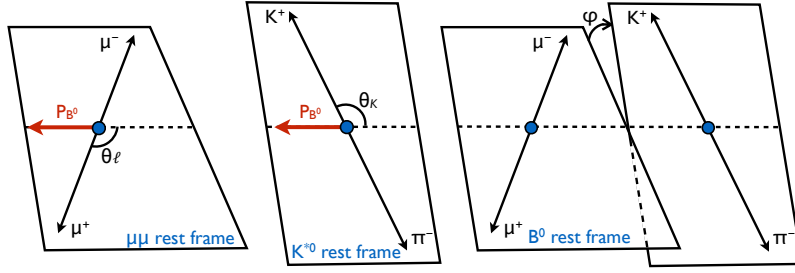


Figure 2: Sketch of the decay $B^0 \rightarrow K^* \mu \mu \rightarrow K^+ \pi^- \mu^+ \mu^-$ with the definition of the three angles describing the final state: $\theta_\ell, \theta_K, \phi$ [25].

Offline reconstruction requires at least two opposite charged muons, and two opposite charged hadrons. The muons are matched with the ones found by the trigger, and the same selection as that at trigger level is applied. In addition the distance from the beamspot must obey $L/\sigma > 3$. The hadrons are required to fail the μ identification criteria and have both $p_T > 0.8 \text{ GeV}$. The distance of closest approach (DCA) of each hadron track with respect to the beamspot has to be $DCA > 2\sigma_{DCA}$. The invariant mass is required to be close to that of the K^* , $|M(K\pi) - M_{K^*}| < 90 \text{ MeV}$. Since CMS has no particle identification capabilities for K and π , both mass hypotheses are used for each tracks. To reduce the ϕ contamination, the invariant mass, computed using the K mass hypothesis for both hadrons, has to be $M_{KK} > 1.035$. The B^0 candidate is reconstructed by fitting the four tracks to a common vertex. A vertex constraint on the momenta is applied. The B^0 candidate has to have $p_t > 8 \text{ GeV}$, $|\eta| < 2.2$, be displaced from the beamspot by $L/\sigma > 12$, with momentum pointing to the beamspot ($\cos \alpha > 0.9994$), and with an invariant mass $|M - M_{B^0}| < 280 \text{ MeV}$. In case of multiple candidates per event, the one with the best B^0 vertex χ^2 is considered. The four-track vertex candidate is identified as a B^0 or \bar{B}^0 depending on which of the $K^+ \pi^-$ or $K^- \pi^+$ invariant masses is closest to the nominal K^* one. The mistag probability is estimated from simulation to be 12-14%, depending on q^2 .

Two control regions are identified for $B^0 \rightarrow J/\psi(\rightarrow \mu\mu)K^*$ and ψ' , based on the dimuon invariant mass $|q - M_{J/\psi(\psi')}| < 3\sigma_M$. A further diagonal band in the plane (M, q) is vetoed in the low side of the control regions in order to reduce the contamination due to unreconstructed soft photons in the charmonium decay. After applying these requirements, 3191 events remain.

The signal contributes to the final state with both P-wave and S-wave, as well as interference between the two. In total, the pdf has 14 parameters: given the available statistics and since we are interested in measuring P_5' , a folding of the pdf is performed around $\phi = 0$ and $\theta_\ell = \pi/2$, reducing the pdf parameters to six, as shown in eq. 3.1.

$$\begin{aligned}
 \frac{1}{d\Gamma/dq^2} \frac{d^4\Gamma}{dq^2 d\cos\theta_\ell d\cos\theta_K d\phi} &= \frac{9}{8\pi} \left\{ \frac{2}{3} \left[(F_S + A_S \cos\theta_K) (1 - \cos^2\theta_\ell) + A_S^2 \sqrt{1 - \cos^2\theta_K} \sqrt{1 - \cos^2\theta_\ell} \cos\phi \right] \right. \\
 &+ (1 - F_S) \left[2F_L \cos^2\theta_K (1 - \cos^2\theta_\ell) + \frac{1}{2} (1 - F_L) (1 - \cos^2\theta_K) (1 + \cos^2\theta_\ell) \right. \\
 &+ \frac{1}{2} P_1 (1 - F_L) (1 - \cos^2\theta_K) (1 - \cos^2\theta_\ell) \cos 2\phi \\
 &\left. \left. + 2P_5' \cos\theta_K \sqrt{F_L(1 - F_L)} \sqrt{1 - \cos^2\theta_K} \sqrt{1 - \cos^2\theta_\ell} \cos\phi \right] \right\}. \quad (3.1)
 \end{aligned}$$

Furthermore, three parameters, F_L , F_S , and A_s , are fixed from the previous measurement, and A_s^5 is treated as a nuisance parameter, leaving only P_1 and P_5' to be measured.

The full pdf has contributions also from mistagged events, as well as from background ones. In order to tell apart signal and background, also the B^0 invariant mass is included in the pdf. The complete unnormalized pdf for each bin in q^2 is shown in eq. 3.2.

$$\begin{aligned} \text{p.d.f.}(m, \cos \theta_K, \cos \theta_l, \phi) = & Y_S^C \cdot \left(S_i^R(m) \cdot S_i^a(\cos \theta_K, \cos \theta_l, \phi) \cdot \varepsilon_i^R(\cos \theta_K, \cos \theta_l, \phi) \right. \\ & \left. + \frac{f_i^M}{1 - f_i^M} \cdot S_i^M(m) \cdot S_i^a(-\cos \theta_K, -\cos \theta_l, -\phi) \cdot \varepsilon_i^M(\cos \theta_l, \cos \theta_K, \phi) \right) \quad (3.2) \\ & + Y_B \cdot B_i^m(m) \cdot B_i^{\cos \theta_K}(\cos \theta_K) \cdot B_i^{\cos \theta_l}(\cos \theta_l) \cdot B_i^\phi(\phi), \end{aligned}$$

where Y_S^C and Y_B are the signal and background yield, respectively, f_i^M is the mistag fraction, and S_i^a is the pdf of eq. 3.1. The pdf for invariant mass $S_i^{R/M}(m)$ are double Gaussians with common mean, the background is evaluated from data side bands, found to be factorizable, and modelled as second- to fourth-order polynomials $B_i^{m, \cos \theta_K, \cos \theta_l}$. The efficiencies $\varepsilon_i^{R/M}(\cos \theta_K, \cos \theta_l, \phi)$ are evaluated from simulated events separately for correctly tagged and mistagged events as a function of the three angles.

An unbinned extended maximum likelihood fit is performed on data, in each bin of q^2 , in two steps. First the background pdf are determined by fitting the invariant mass side bands. These pdf are then fixed for the second step, where a fit on the full mass range is performed. This second step is performed by discretizing the P_1, P_5' space, maximizing the likelihood \mathcal{L} as a function of the three remaining nuisance parameters Y_S^C , Y_B , and A_s^5 , and finally fitting the \mathcal{L} with a bivariate Gaussian in order to find the absolute maximum inside the physical domain, where the pdf is always positive defined. The statistical uncertainties of the results are evaluated using the Feldman–Cousins method [33] with nuisance parameters. Two main sets of pseudo-experimental samples are generated. The first (second) set, used to compute the coverage for P_1 (P_5'), is generated by assigning values to the other parameters as obtained by profiling the bivariate Gaussian distribution description of the likelihood determined from data at fixed P_1 (P_5') values. When fitting the pseudo-experimental samples, the same fit procedure as applied to the data is used. The fit formalism and results are validated through fits to pseudo-experimental samples, MC simulation samples, and control channels.

Systematic uncertainties include effects from simulation mis-modeling, fit bias, limited amount of simulated data, efficiency shape, mistag probability, background distribution, mass distribution, angular resolution effect, and feed-through background from control regions. These are evaluated from high statistics simulated events, pseudo-experiment constructed combining simulated signal with background from data side bands, fit on control regions, and propagation, via pseudo experiment, of other uncertainties.

An important systematics is due to the usage of fixed values of F_L , F_S , and A_s from previous measurement on the same dataset. This has been evaluated via pseudo-experiment with statistics larger than data, by comparing a full fit with the three parameter fixed and free to float. No bias has been found, and the comparison of the statistical uncertainties on P_1 and P_5' in the two fits are used to assign the systematics uncertainties. The stability of the ratio of the two statistical uncertainties as a function of the pseudo-experiment statistics has been also verified. Furthermore, a fully free fit on the two control regions shows no bias in the determination of P_1 and P_5' .

The final yield in all seven bins is 1397 signal and 1794 background events. The results on P_1 and P_5' are shown in fig. 3, where also the results published by LHCb [20] and Belle [22] collaborations are shown. Two SM predictions, denoted SM-DHNV and SM-HEPfit, are available for comparison with the measured angular parameters. The SM-DHNV result, derived from Refs. [8, 13], updates the calculations from Ref. [34] to account for the known correlation between the different form factors [35]. It also combines predictions from light-cone sum rules, which are valid in the low- q^2 region, with lattice predictions at high q^2 [36] to obtain more precise determinations of the form factors over the full q^2 range. The hadronic charm quark loop contribution is obtained from Ref. [37]. The SM-HEPfit result, derived from Refs. [38, 39], uses full QCD form factors [35] and obtains the hadronic contribution from LHCb data [20]. Both sets of predictions are seen to be in agreement with the CMS results, although the agreement with the SM-DHNV prediction is somewhat better. There is thus no evidence for physics beyond the SM. Qualitatively, the CMS measurements are compatible with the LHCb results. The Belle measurements lie systematically above both the CMS and LHCb results and the SM predictions.

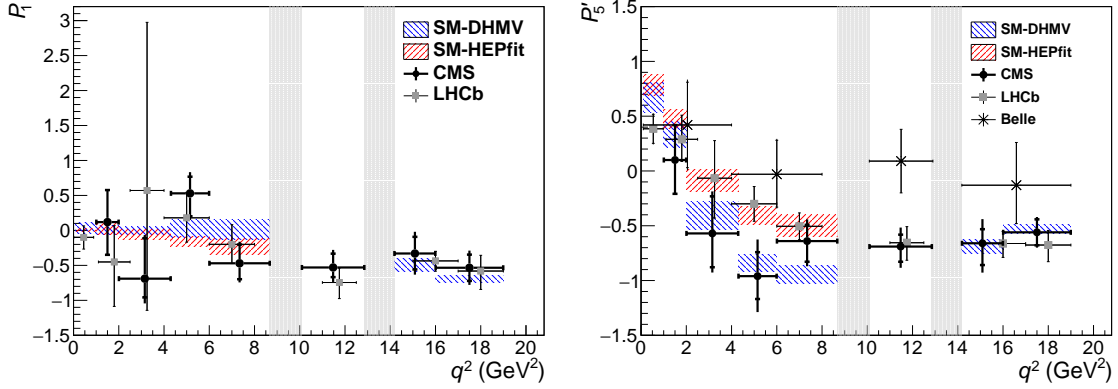


Figure 3: CMS measurements [25] of the P_1 and P_5' angular variables versus q^2 for $B^0 \rightarrow K^* \mu \mu$ decays, in comparison to results from the LHCb [20] and Belle [22] Collaborations. The statistical uncertainties are shown by the inner vertical bars, while the outer vertical bars give the total uncertainties. The horizontal bars show the bin widths. The vertical shaded regions correspond to the J/ψ and ψ' resonances. The hatched regions show the predictions from two SM calculations described in the text, averaged over each q^2 bin.

4. Summary

We have presented results on the measurement of $\mathcal{B}(B_s^0(B^0) \rightarrow \mu \mu)$ branching fraction and angular parameters P_1 and P_5' for the $B^0 \rightarrow K^* \mu \mu$ decay using pp collisions with CMS detector at LHC run 1, at $\sqrt{s} = 7$ and 8 TeV. The significance for $\mathcal{B}(B_s^0)$ is 4.3σ (6.2 together with LHCb), and that for B^0 is 3.2σ (combining the two experiments): the values are compatible with SM prediction. The P_1 and P_5' have been measured with good precision as a function of q^2 with 1400 signal events, and are found to be consistent with predictions based on the standard model. The results are among the most precise to date.

References

- [1] C. Bobeth, M. Gorbahn, T. Hermann, M. Misiak, E. Stamou et al., $B_{s,d} \rightarrow \ell^+ \ell^-$ in the Standard Model with Reduced Theoretical Uncertainty, *Phys. Rev. Lett.* **112** (2014) 101801, [1311.0903].
- [2] J. Ellis, K. A. Olive, Y. Santoso and V. C. Spanos, On $B_s \rightarrow \mu\mu$ and cold dark matter scattering in the MSSM with non-universal higgs masses, *JHEP* **2006** (2006) 063.
- [3] S. Davidson and S. Descotes-Genon, “minimal flavour violation” for leptoquarks, *JHEP* **2010** (Nov, 2010) 73.
- [4] J. R. Ellis, J. S. Lee and A. Pilaftsis, B-Meson Observables in the Maximally CP-Violating MSSM with Minimal Flavour Violation, *Phys. Rev.* **D76** (2007) 115011, [0708.2079].
- [5] S. R. Choudhury, A. S. Cornell, N. Gaur and G. C. Joshi, Signatures of new physics in dileptonic b-decays, *Int. J. Mod. Phys. A* **21** (2006) 2617–2634.
- [6] W. Altmannshofer, P. Ball, A. Bharucha, A. J. Buras, D. M. Straub and M. Wick, Symmetries and asymmetries of $B \rightarrow K^* \mu^+ \mu^-$ decays in the Standard Model and beyond, *JHEP* **01** (2009) 019, [0811.1214].
- [7] F. Krüger and J. Matias, Probing new physics via the transverse amplitudes of $B^0 \rightarrow K^{*0} (\rightarrow K^- \pi^+) \ell^+ \ell^-$ at large recoil, *Phys. Rev. D* **71** (2005) 094009, [hep-ph/0502060].
- [8] S. Descotes-Genon, J. Matias, M. Ramon and J. Virto, Implications from clean observables for the binned analysis of $B \rightarrow K^* \mu^+ \mu^-$ at large recoil, *JHEP* **01** (2013) 048, [1207.2753].
- [9] C. Bobeth, G. Hiller and D. van Dyk, General analysis of $\bar{B} \rightarrow \bar{K}^{(*)} \ell^+ \ell^-$ decays at low recoil, *Phys. Rev. D* **87** (2012) 034016, [1212.2321].
- [10] A. Ali, G. Kramer and G. Zhu, $B \rightarrow K^* \ell^+ \ell^-$ decay in soft-collinear effective theory, *Eur. Phys. J. C* **47** (2006) 625, [hep-ph/0601034].
- [11] W. Altmannshofer, P. Paradisi and D. M. Straub, Model-independent constraints on new physics in $b \rightarrow s$ transitions, *JHEP* **04** (2012) 008, [1111.1257].
- [12] S. Jäger and J. Martin Camalich, On $B \rightarrow V \ell \ell$ at small dilepton invariant mass, power corrections, and new physics, *JHEP* **05** (2013) 043, [1212.2263].
- [13] S. Descotes-Genon, T. Hurth, J. Matias and J. Virto, Optimizing the basis of $B \rightarrow K^* \ell^+ \ell^-$ observables in the full kinematic range, *JHEP* **05** (2013) 137, [1303.5794].
- [14] BaBar Collaboration, Angular distributions in the decay $B \rightarrow K^* \ell^+ \ell^-$, *Phys. Rev. D* **79** (2009) 031102, [0804.4412].
- [15] BABAR collaboration, Belle Collaboration, Measurement of the differential branching fraction and forward-backward asymmetry for $B \rightarrow K^{(*)} \ell^+ \ell^-$, *Phys. Rev. Lett.* **103** (2009) 171801, [0904.0770].
- [16] CDF Collaboration, Measurements of the angular distributions in the decays $B \rightarrow K^{(*)} \mu^+ \mu^-$ at CDF, *Phys. Rev. Lett.* **108** (2012) 081807, [1108.0695].
- [17] LHCb Collaboration, Differential branching fraction and angular analysis of the decay $B^0 \rightarrow K^{*0} \mu^+ \mu^-$, *JHEP* **08** (2013) 131, [1304.6325].
- [18] CMS Collaboration, Angular analysis and branching fraction measurement of the decay $B^0 \rightarrow K^{*0} \mu^+ \mu^-$, *Phys. Lett. B* **727** (2013) 77, [1308.3409].
- [19] CMS Collaboration, Angular analysis of the decay $B^0 \rightarrow K^{*0} \mu^+ \mu^-$ from pp collisions at $\sqrt{s} = 8$ TeV, *Phys. Lett. B* **753** (2016) 424, [1507.08126].

- [20] LHCb Collaboration, *Angular analysis of the $B^0 \rightarrow K^* \mu^+ \mu^-$ decay using 3 fb^{-1} of integrated luminosity*, *JHEP* **02** (2016) 104, [1512.04442].
- [21] S. Descotes-Genon, J. Matias and J. Virto, *Global analysis of $b \rightarrow s \ell \ell$ anomalies*, *JHEP* **06** (2016) 092, [1510.04239].
- [22] Belle Collaboration, *Lepton-Flavor-Dependent angular analysis of $B \rightarrow K^* \ell^+ \ell^-$* , *Submitted to Phys. Rev. Lett.* (2017), [1612.05014].
- [23] CMS Collaboration, *Measurement of the $B_s^0 \rightarrow \mu^+ \mu^-$ branching fraction and search for $B^0 \rightarrow \mu^+ \mu^-$ with the cms experiment*, *Phys. Rev. Lett.* **111** (Sep, 2013) 101804.
- [24] LHCb, CMS Collaborations, *Observation of the rare $B_s^0 \rightarrow \mu^+ \mu^-$ decay from the combined analysis of CMS and LHCb data*, *Nature* **522** (2015) 68–72, [1411.4413].
- [25] CMS Collaboration, *Measurement of the P_1 and P_5' angular parameters of the decay $B^0 \rightarrow K^{*0} \mu^+ \mu^-$ in proton-proton collisions at $\sqrt{s} = 8 \text{ TeV}$* , Tech. Rep. CMS-PAS-BPH-15-008, CERN, Geneva, 2017.
- [26] CMS Collaboration, *Angular analysis of the decay $b_0 \rightarrow K^* 0 \mu^+ \mu^-$ from pp collisions at $\sqrt{s} = 8 \text{ tev}$* , *Physics Letters B* **753** (2016) 424 – 448.
- [27] CMS collaboration, *The CMS experiment at the CERN LHC*, *JINST* **3** (2008) S08004.
- [28] LHCb Collaboration, *Measurement of the fragmentation fraction ratio f_s/f_d and its dependence on b meson kinematics*, *JHEP* **2013** (Apr, 2013) 1.
- [29] LHCb Collaboration, *Measurement of the $B_s^0 \rightarrow \mu^+ \mu^-$ branching fraction and search for $B^0 \rightarrow \mu^+ \mu^-$ decays at the LHCb experiment*, *Phys. Rev. Lett.* **111** (Sep, 2013) 101805.
- [30] ATLAS Collaboration, *Study of the rare decays of B_s^0 and B^0 into muon pairs from data collected during the LHC Run 1 with the ATLAS detector*, *Eur. Phys. J. C* **76** (Sep, 2016) 513.
- [31] LHCb Collaboration, *Measurement of the $B_s^0 \rightarrow \mu^+ \mu^-$ branching fraction and effective lifetime and search for $B^0 \rightarrow \mu^+ \mu^-$ decays*, *Phys. Rev. Lett.* **118** (May, 2017) 191801.
- [32] J. Matias, F. Mescia, M. Ramon and J. Virto, *Complete anatomy of $\bar{B}_d \rightarrow \bar{K}^{*0} (\rightarrow K \pi) \ell^+ \ell^-$ and its angular distribution*, *JHEP* **04** (2012) 104, [1202.4266].
- [33] G. J. Feldman and R. D. Cousins, *Unified approach to the classical statistical analysis of small signals*, *Phys. Rev. D* **57** (1998) 3873, [physics/9711021].
- [34] P. Ball and R. Zwicky, *$B_{d,s} \rightarrow \rho, \omega, K^*, \phi$ decay form factors from light-cone sum rules reexamined*, *Phys. Rev. D* **71** (2005) 014029, [hep-ph/0412079].
- [35] A. Bharucha, D. M. Straub and R. Zwicky, *$b \rightarrow \nu \ell^+ \ell^-$ in the standard model from light-cone sum rules*, *JHEP* **08** (2016) 098, [1503.05534].
- [36] R. R. Horgan, Z. Liu, S. Meinel and M. Wingate, *Lattice QCD calculation of form factors describing the rare decays $B \rightarrow K^* \ell^+ \ell^-$ and $B_s \rightarrow \phi \ell^+ \ell^-$* , *Phys. Rev. D* **89** (2014) 094501, [1310.3722].
- [37] A. Khodjamirian, T. Mannel, A. A. Pivovarov and Y.-M. Wang, *Charm-loop effect in $B \rightarrow K^{(*)} \ell^+ \ell^-$ and $b \rightarrow K^* \gamma$* , *JHEP* **09** (2010) 089, [1006.4945].
- [38] M. Ciuchini, M. Fedele, E. Franco, S. Mishimad, A. Paul, L. Silvestrini et al., *$B \rightarrow K^* \ell^+ \ell^-$ decays at large recoil in the Standard Model: a theoretical reappraisal*, *JHEP* **06** (2016) 116, [1512.07157].
- [39] M. Ciuchini, M. Fedele, E. Franco, S. Mishimad, A. Paul, L. Silvestrini et al., *$B \rightarrow K^* \ell^+ \ell^-$ in the Standard Model: elaborations and interpretations*, *Proceedings of the 38th International Conference on High Energy Physics, 3-10 August 2016, Chicago, USA* (2016), [1611.04338].